

# The Nitrogen Conundra for Old Stellar Populations

David Burstein

Arizona State University

in collaboration with

Yong Li (ASU)

Mike Bessell, Ken Freeman, John Norris (ANU),

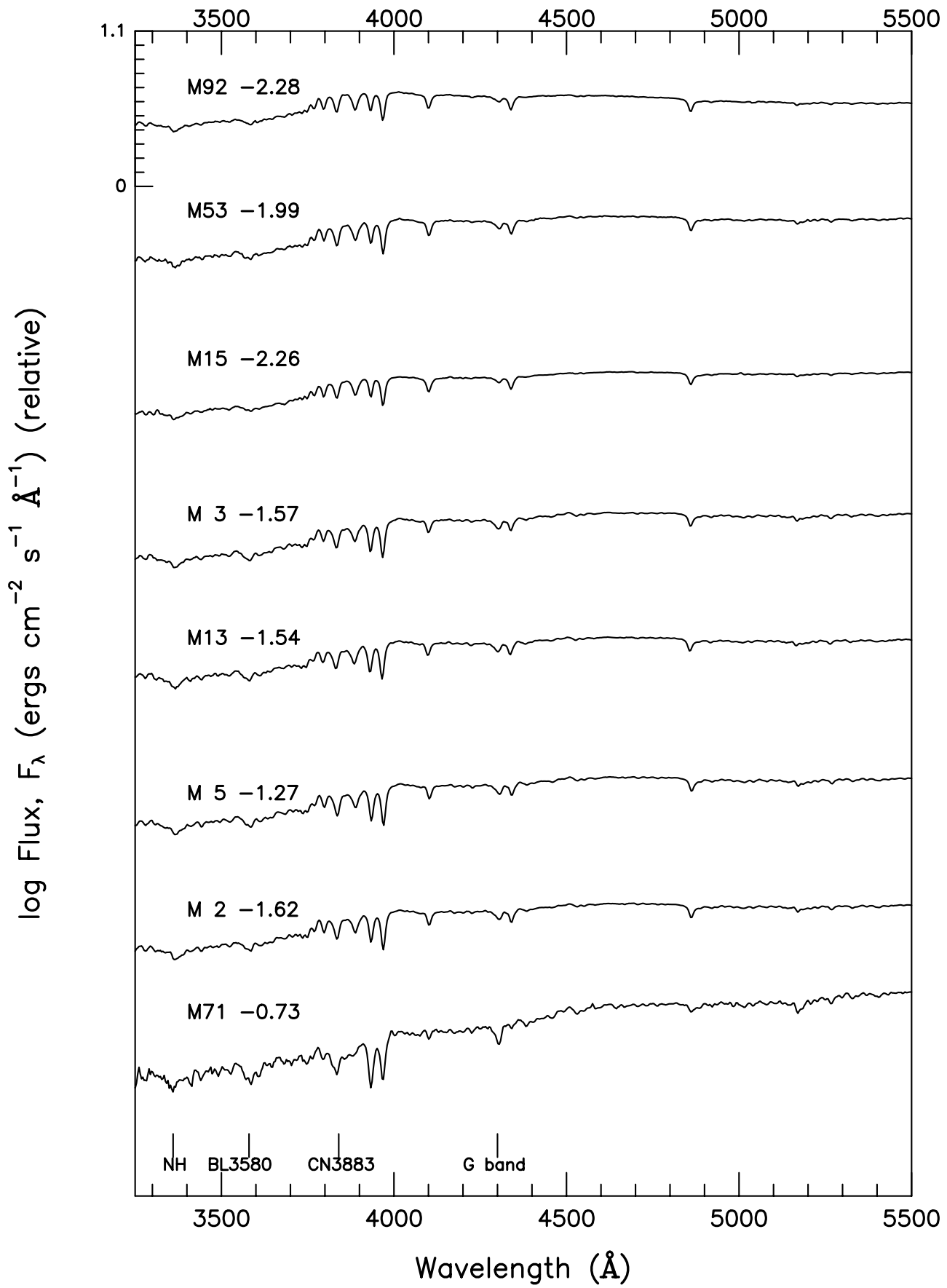
Joss Bland–Hawthorn, Russell Cannon (AAO),

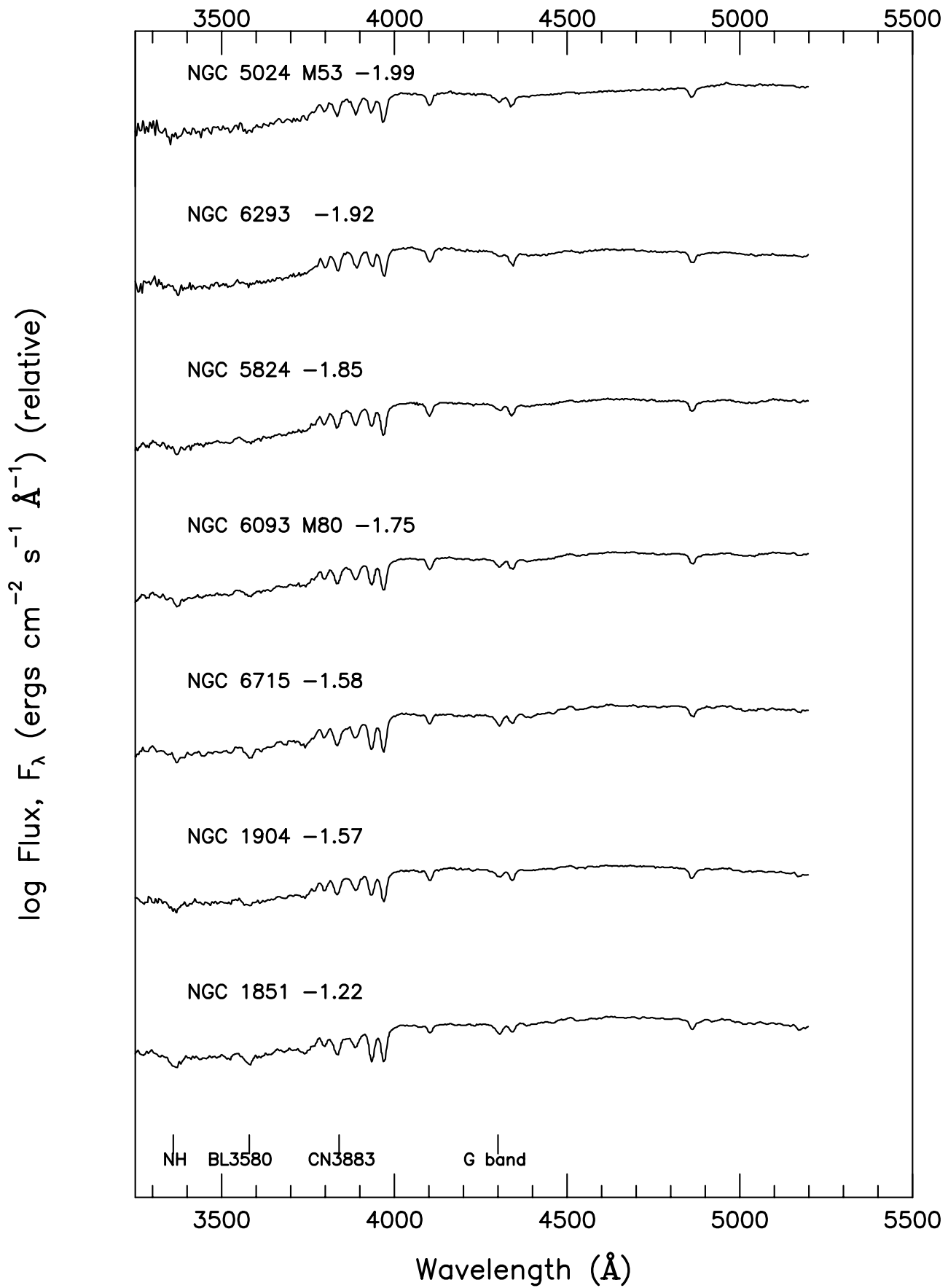
Brad Gibson, Michael Beasley, and

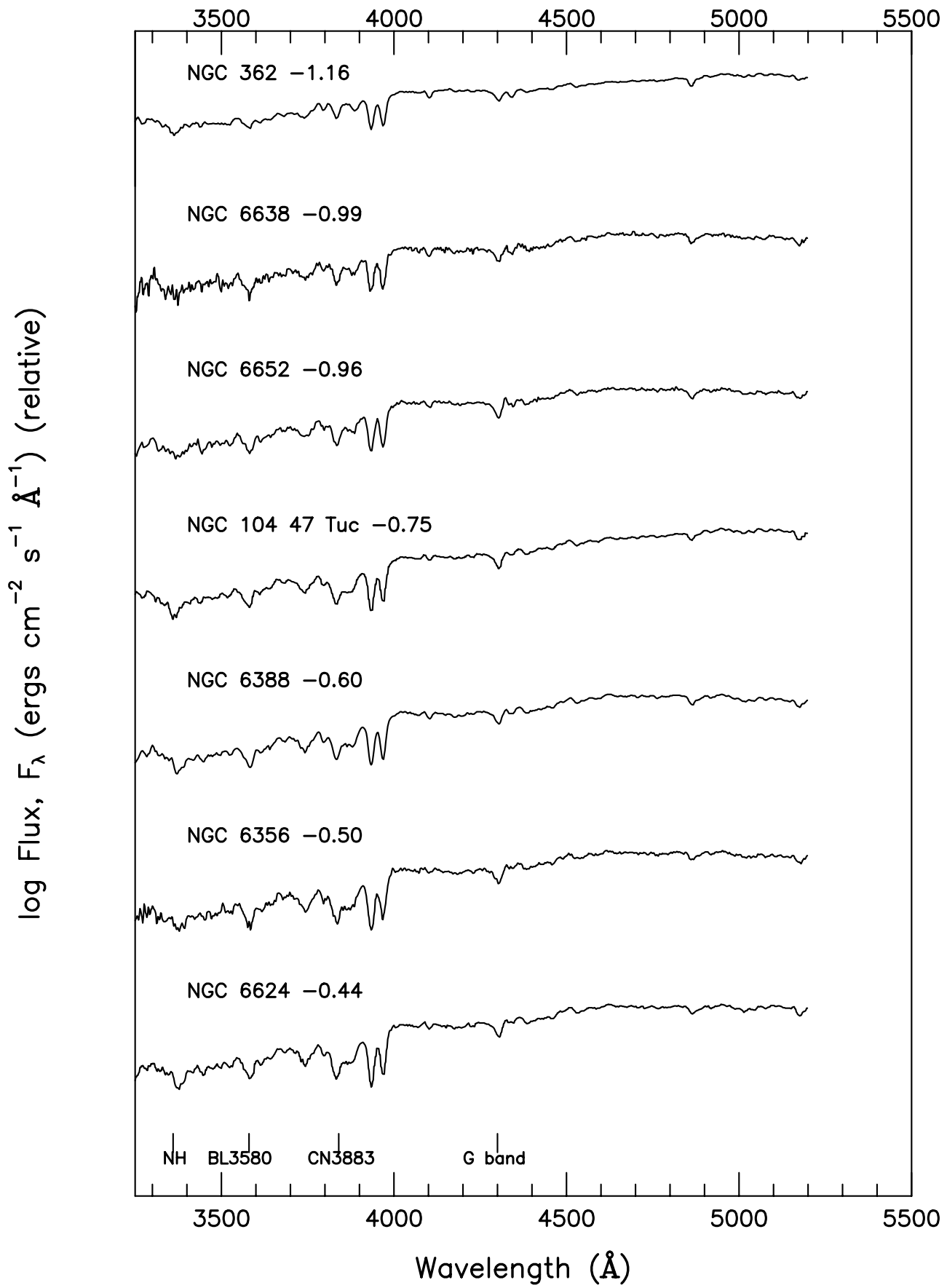
Hyun–chul Lee (Swinburne, Melbourne),

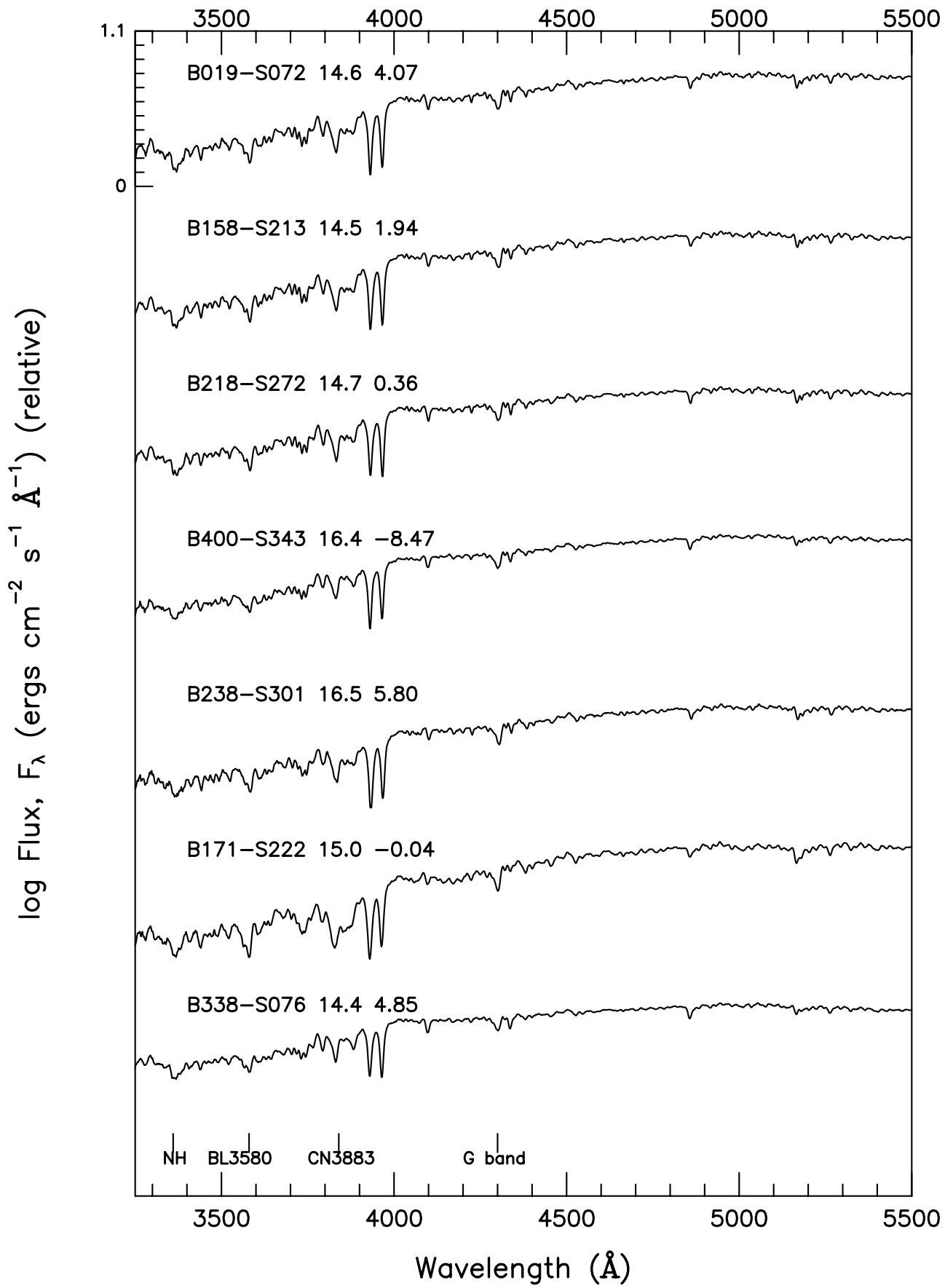
and Beatriz Barbuy (Sao Paulo)

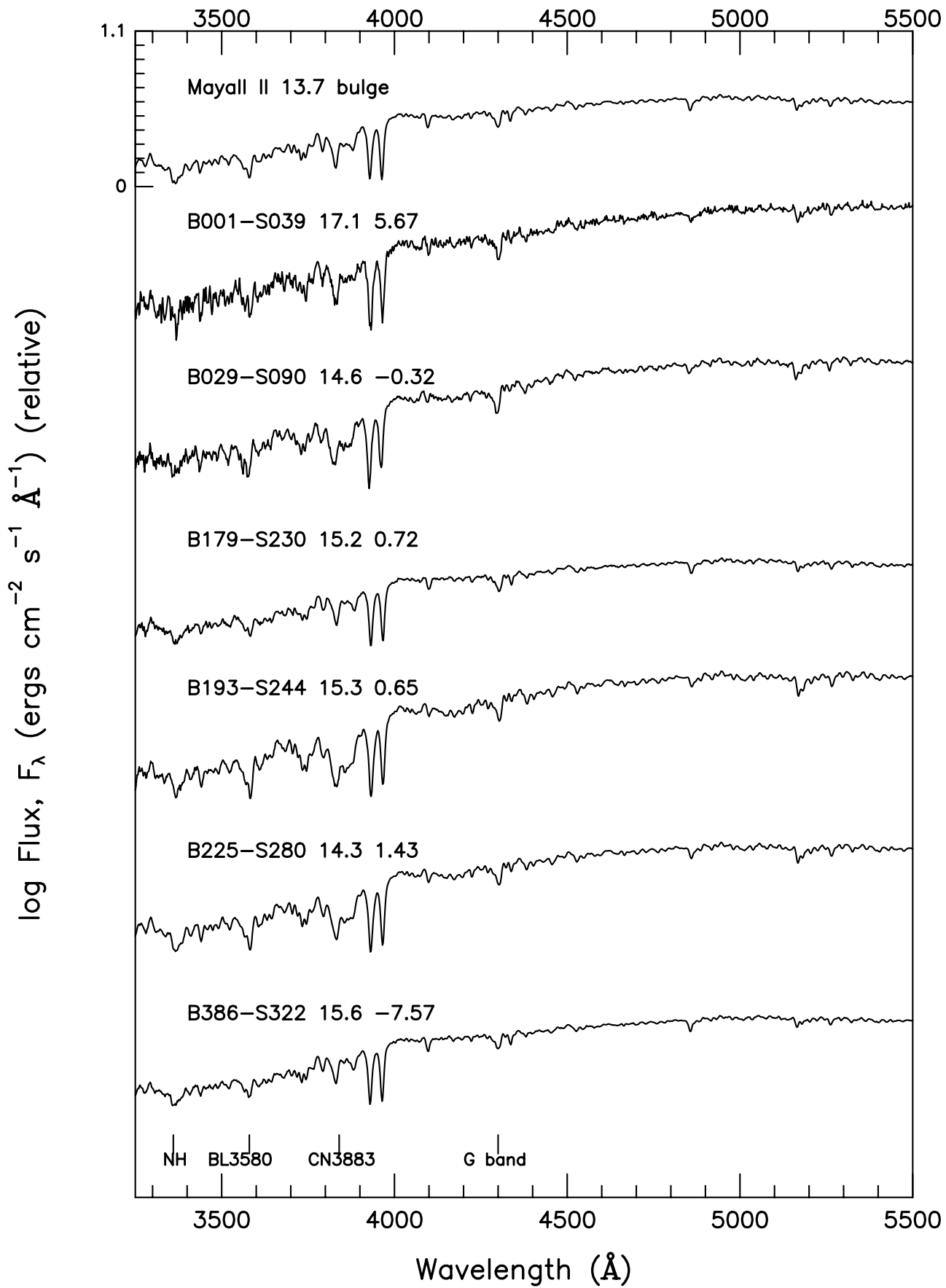
Our group has obtained spectra from 3250Å to 6000Å for 8 Galactic globular clusters (GC), 22 M31 GCs, and for his Ph.D. thesis, Yong Li has obtained similar spectra for 125 Galactic stars, dwarfs and giants. Bica, Alloin and Schmidt (1994, A&A, 283, 505) also published spectra from 3250Å for 14 more Galactic GCs. Here I show our spectra for the old GCs in our Galaxy and in M31 (yes, there are also young GCs in M31, but that is another story; see Burstein et al., 2004, ApJ, 614, 158). Then we show the line indices we measure for these GC and stars, then the results of those measurements.











From the stellar data, we have defined a mean Fe index ( $\langle \text{Fe} \rangle$ ) from nine individual Fe lines (at 4383, 4531, 4668, 5015, 5270, 5335, 5460, 5709 and 5782Å) that is an indication of the Fe–line strength of both the stars and the GCs. We then also define indices to measure NH, CN, CH (the G–band), Ca II H+K, H $\beta$ , Tio1, Tio2, MgH, Mg, Ca, and Na in both the stars and GCs.

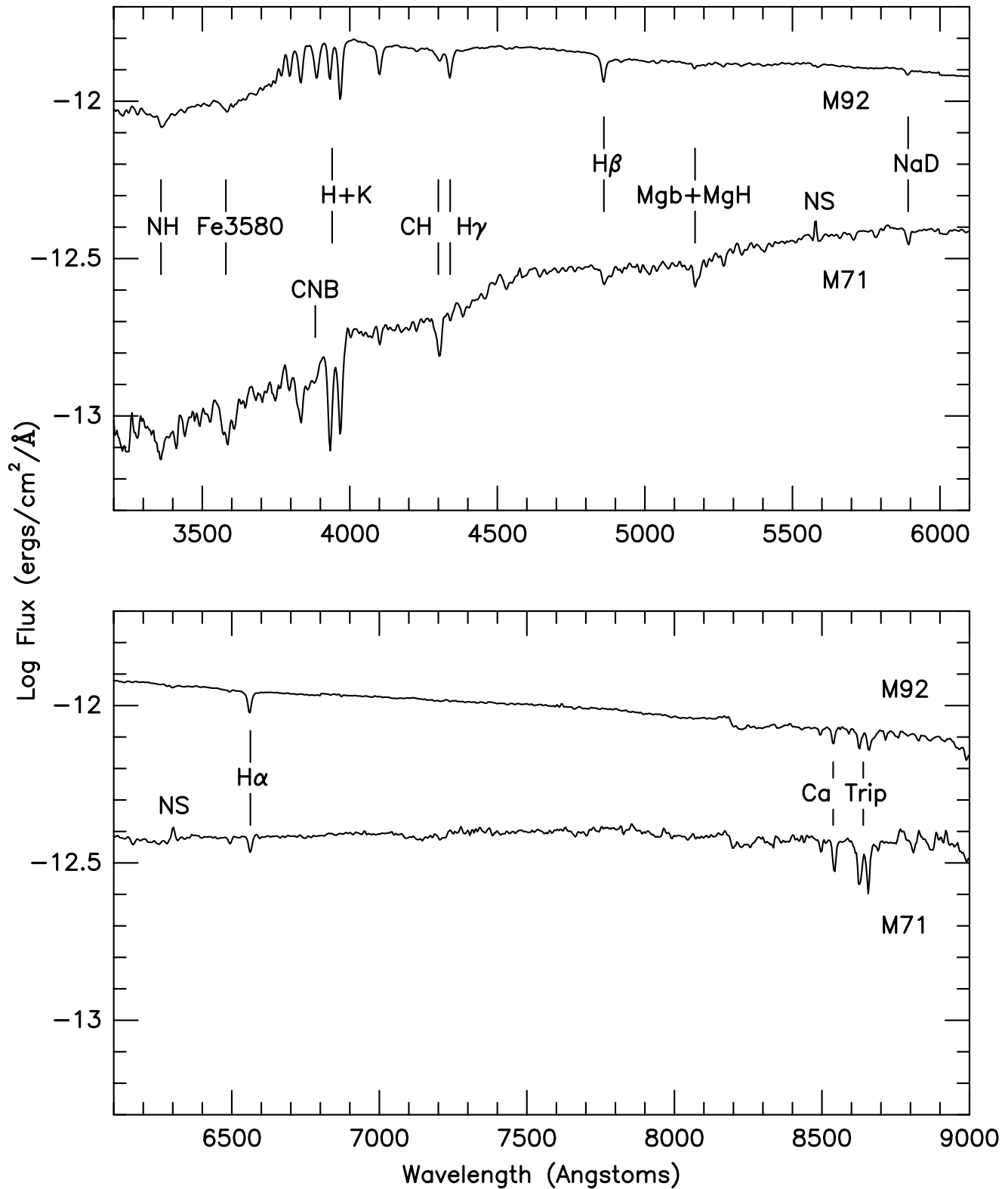


Figure 1. The spectra taken by Yong Li of the metal-poor GC M92 (upper spectrum) and of the metal-rich GC M71 (lower spectrum) with the principal line indices noted. Note the high S/N of these spectra, indicative of the high quality data acquired by Li.

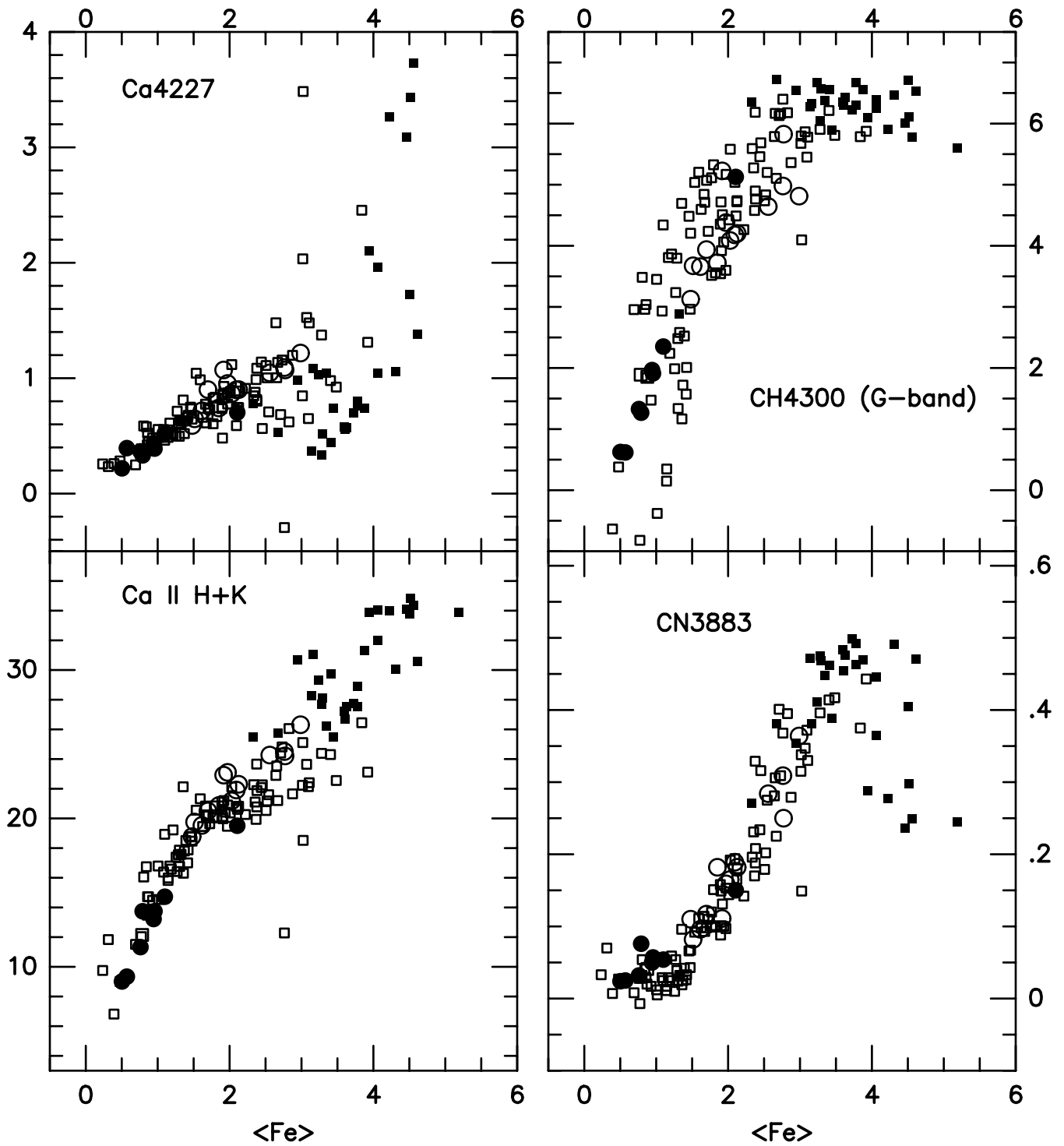


Figure 2. Line index relationships for dwarf stars (small open squares), giant stars (small closed squares), 8 Galactic GC from Li's Ph.D. thesis (large closed circles); 14 old M31 GCs (large open circles) and 2, 5-Gyr-old M31 GCs (large open squares). Each line index (indicated in each of the four graphs) is plotted vs. our  $\langle Fe \rangle$  index for uniformity.

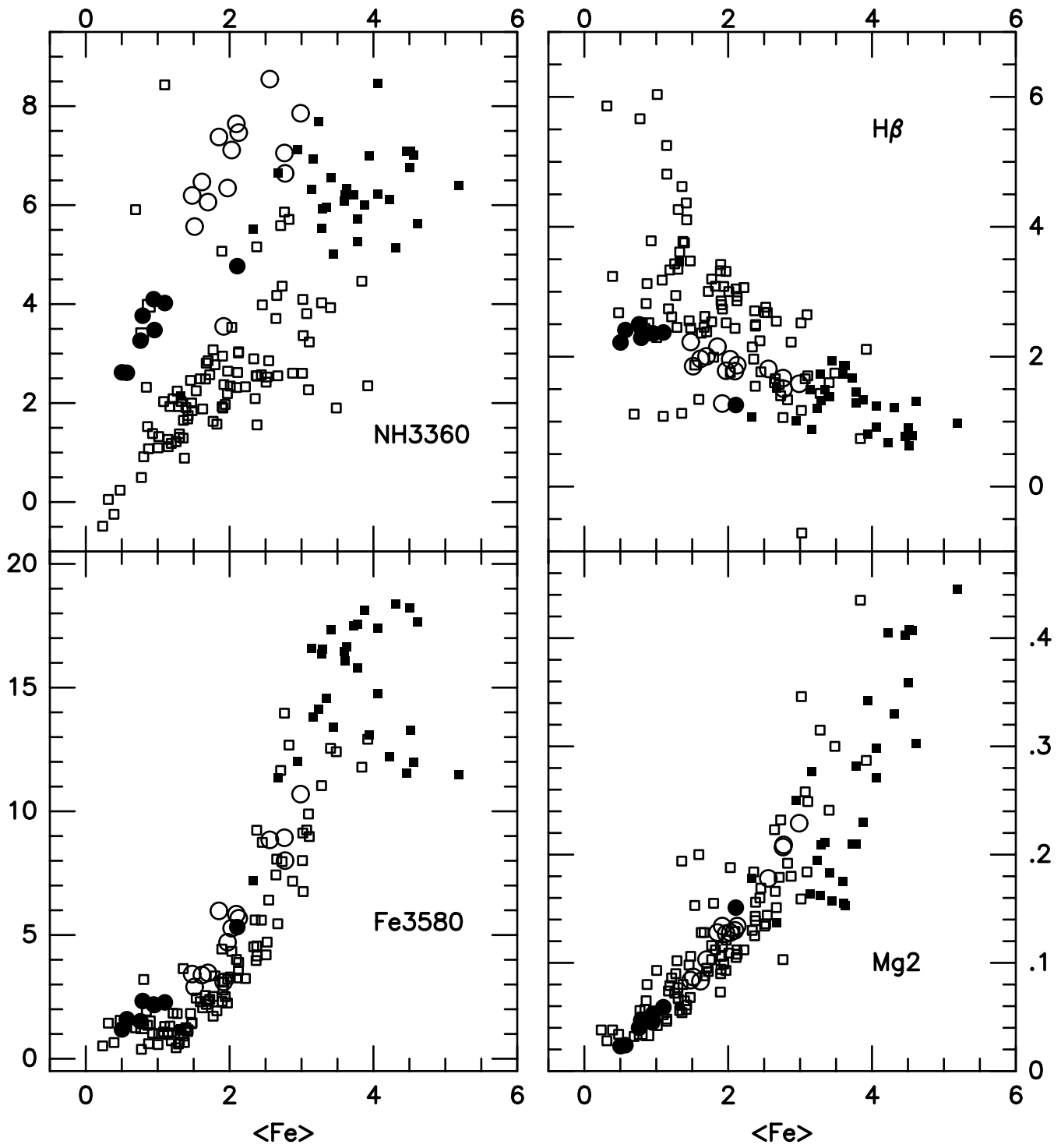


Figure 3. Same data plotted as in Figure 2. All graphs plotted vs our  $\langle \text{Fe} \rangle$  index, with the index plotted labeled in the graph.

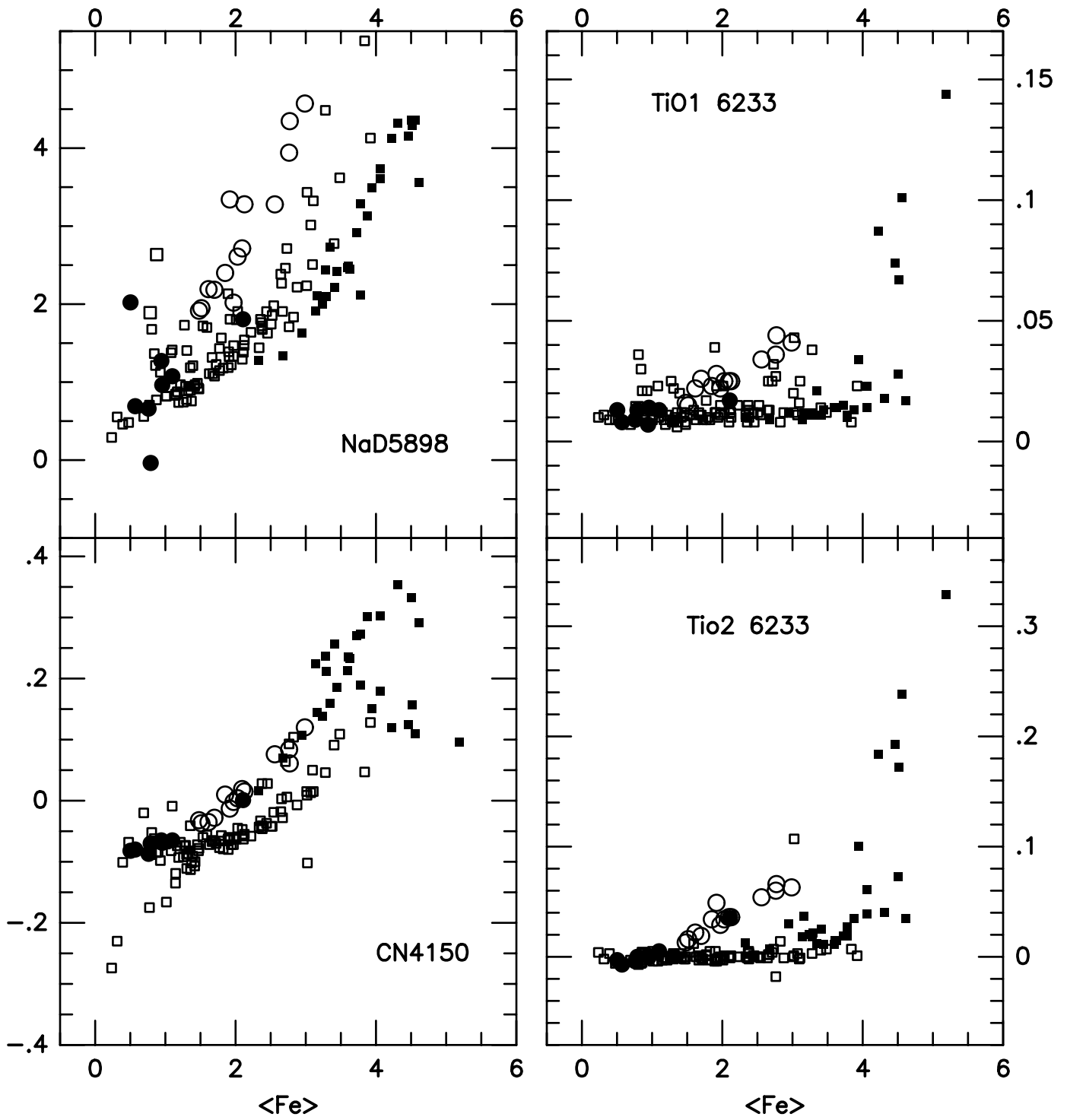


Figure 4. Same data as plotted in Figures 2 and 3, plotted in the same manner as in those figures.

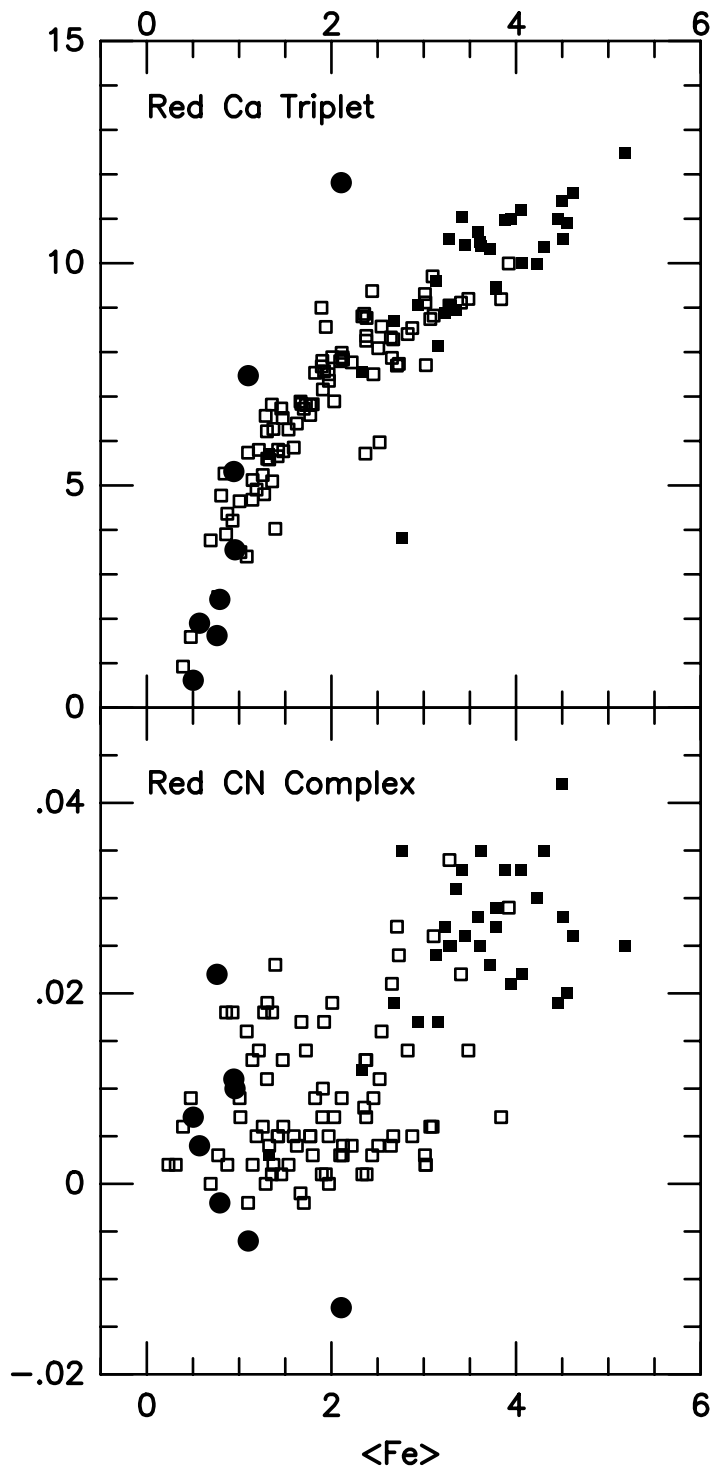


Figure 5. Two of the red features in our Galactic stars and our Galactic GC observations (M31 GC do not yet have red observations.)

In contrast to what we see in the old GCs in both M31 and our Galaxy (only nitrogen is overabundant), what others see in the most metal-poor stars in the Galactic halo is different. Here I show the results published by Frebel et al. (including some of our collaboration) in Nature, 2005, 434, 871 for two  $[Fe/H] \sim -5.5$  stars.

Table 1 Abundance ratios of HE1327–2326

| Element      | [X/Fe], A(Li), [Fe/H] |            |
|--------------|-----------------------|------------|
|              | Subgiant              | Dwarf      |
| Li           | <1.6                  | <1.6       |
| C            | 4.1 ± 0.2             | 3.9 ± 0.2  |
| N            | 4.5 ± 0.2             | 4.2 ± 0.2  |
| O            | <4.0                  | <3.7       |
| Na (LTE)     | 2.4 ± 0.2             | 2.4 ± 0.2  |
| Na (non-LTE) | 2.0 ± 0.2             | 2.0 ± 0.2  |
| Mg (LTE)     | 1.7 ± 0.2             | 1.7 ± 0.2  |
| Mg (non-LTE) | 1.6 ± 0.2             | 1.6 ± 0.2  |
| Al (LTE)     | 1.3 ± 0.2             | 1.3 ± 0.2  |
| Al (non-LTE) | 1.7 ± 0.2             | 1.7 ± 0.2  |
| Ca I         | 0.1 ± 0.2             | 0.1 ± 0.2  |
| Ca II        | 0.9 ± 0.2             | 0.8 ± 0.2  |
| Ti           | 0.6 ± 0.2             | 0.8 ± 0.2  |
| Fe (LTE)     | −5.6 ± 0.2            | −5.7 ± 0.2 |
| Fe (non-LTE) | −5.4 ± 0.2            | −5.5 ± 0.2 |
| Sr (LTE)     | 1.0 ± 0.2             | 1.2 ± 0.2  |
| Sr (non-LTE) | 1.1 ± 0.2             | 1.3 ± 0.2  |
| Ba (LTE)     | <1.4                  | <1.7       |
| Ba (non-LTE) | <1.4                  | <1.7       |

Using colour- $T_{\text{eff}}$  relations<sup>24</sup>, we determine  $T_{\text{eff}} = 6,180 \pm 80$  K from broad-band UBVR $I$  photometry obtained with the MAGNUM telescope<sup>25</sup>, Hawaii, and JHK magnitudes taken from the 2MASS survey<sup>26</sup>. To constrain the gravity ( $\log g$ ), we use the proper motion<sup>27</sup> ( $\mu = 0.073 \pm 0.006$  arcsec yr<sup>-1</sup>) of HE1327–2326 to set limits on its distance (assuming that the Galactic escape velocity is  $500 \text{ km s}^{-1}$  and larger than the transverse velocity). It follows that the absolute  $V$  magnitude is  $M_V > 2.7$  mag which constrains the evolutionary status of the star and therefore  $\log g$ . Inspection of a 12-billion-year isochrone with  $[\text{Fe}/\text{H}] = -3.5$  (the most metal-poor one available<sup>28</sup>) results in two solutions for the surface gravity  $\log g$ : 3.7 and 4.5 (in cgs units). Owing to weak observational constraints on  $\log g$ , it is currently not possible to determine which of these solutions is correct.  $T_{\text{eff}}$  and  $\log g$  are the input for two different plane-parallel LTE model atmospheres that we use to derive the abundances for both gravity solutions; a MARCS model (Gustafsson, B. *et al.*, manuscript in preparation) tailored for the chemical composition of HE1327–2326, and a Kurucz model<sup>29</sup>. Both sets of abundances agree to within 0.1 dex. Using spectrum synthesis we determine the C and N abundances from CH and NH molecular bands and the upper limit for O from OH molecular bands in the ultraviolet spectral range. Apart from the molecular features, only 13 weak absorption lines are detected in spectral regions not affected by the wings of the Balmer lines and thus suitable for our abundance analysis. Solar abundances were taken from ref. 30. Typical statistical 1 $\sigma$  errors in our abundances are 0.2 dex. Possible systematic errors are judged to be of the same order of magnitude. Non-LTE corrections are included where available<sup>22</sup>. For the calculation of the non-LTE abundance ratios, the non-LTE iron abundance has been used.

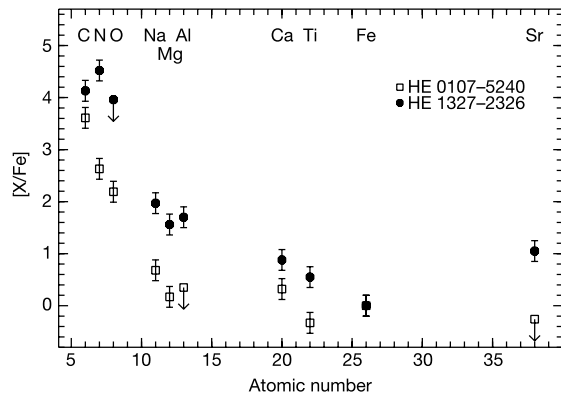


**Figure 2** Abundance patterns of HE1327–2326 (subgiant solution, filled circles) and HE1017–5240 (open squares). Typical 1- $\sigma$  errors of 0.2 dex are shown in the plot. Upper limits are indicated by an arrow. We adopt the same non-LTE corrections for both stars<sup>22</sup>, which lead to the modification of the published abundances of HE01017–5240. Consequently, we adopt  $[\text{Fe}/\text{H}]_{\text{non-LTE}} = -5.2$  (ref. 9) as the iron abundance for HE01017–5240. These two most Fe-poor stars both have very large C enhancement relative to Fe by a factor of  $\sim 5,000$  (HE01017–5240) and  $\sim 10,000$  (HE1327–2326).  $N/\text{Fe}$  is  $\sim 30,000$  times the solar value (considering the subgiant solution) in HE1327–2326 whereas it is  $\sim 200$  times the solar value in HE01017–5240. The upper limit for the O abundance of HE1327–2326 is  $[\text{O}/\text{Fe}] < 4.0$ . Oxygen in HE01017–5240 has recently been determined<sup>23</sup> to be  $[\text{O}/\text{Fe}] = 2.3$ , which is of the same order as its  $[\text{N}/\text{Fe}]$  value. These enormous overabundances in CNO elements suggest that both stars belong to a group of objects sharing a common formation scenario. HE1327–2326 and HE01017–5240 have Ca/Fe and Ti/Fe abundance ratios that are enhanced by factors of less than ten compared to the Sun. The light-element ratios Na/Fe, Mg/Fe and Al/Fe, as well as, surprisingly, Sr/Fe, are all enhanced by factors of  $\sim 10$  to  $\sim 100$  in HE1327–2326. Of these four elements, only Na and Mg are detected in HE01017–5240 with element/Fe ratios close to the solar value. As for several other elements, an upper limit for Ba has been measured in both stars. The Sr/Ba ratio is crucial to identify the origin for the Sr and other heavy elements.

The overabundance of nitrogen in these old GCs comes from their main sequence stars. This is seen in the most metal-poor GCs, which do not show a hint of red giant lights, as well as in the study of Briley, Harbeck, Smith and Grebel, 2004, AJ, 127, 1588, who obtained C and N abundances for main sequence stars in 47 Tuc, and also show the results of other studies of subgiant and giant stars of M71 and M5.

Smith, Briley and Harbeck (2005, AJ, 129 1589) find similar results for the giants in M13, M10 and NGC 7006.

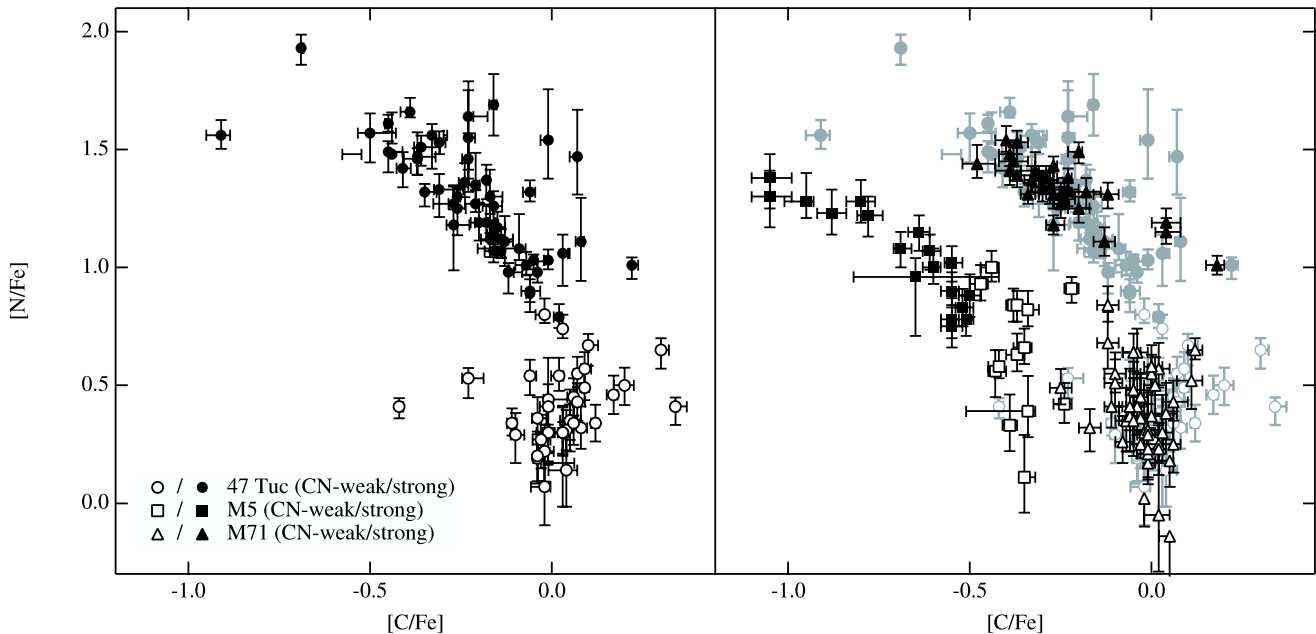


FIG. 4.—Resulting C and N abundances measured by matching CH and CN band strengths plotted against each other. *Left*: Only the results for the present sample of 47 Tuc MS stars are shown, where the strong anticorrelation between C and N can be seen among the CN-strong stars. In contrast, the CN-weak stars exhibit only a modest range in  $[C/Fe]$ . *Right*: The distribution of C and N among a similar sample of M71 and M5 stars (from Briley et al. 2002 and Cohen et al. 2002) is also plotted. The general pattern (i.e., a C/N anticorrelation) is the same between all three clusters, and M71 and 47 Tuc (two clusters of similar metallicity) appear to be essentially indistinguishable. In the case of the more metal-poor M5, the C depletions are more extreme, yet the N enhancements are not.

Hence, the two conundra we can define that involve nitrogen and old stellar populations are these:

1. Why do M31 GCs have higher nitrogen abundances than Galactic GC at equivalent metallicities?
2. Why do a subset of very metal-poor Galactic halo stars see CNO overabundances but we do not see C overabundance in GCs?

## Consequences:

1. Either halo stars did not form from dissolved GCs or if they did, these are not the GCs we see today.

2. Whence nitrogen? To solve this riddle, we will have to understand how the halo of our Galaxy and of other galaxies formed, perhaps involving the zero-metal stars that first formed.